Supplemental Material

Direct Cell Mass Measurements Expand the Role of Small Microorganisms in Nature

Alexander Khachikyan[a], Jana Milucka[a#], Sten Littmann[a], Soeren Ahmerkamp[a,b], Travis Meador[b,c], Martin Könneke[b], Thomas Burg[d] and Marcel M. M. Kuypers[a]

[a] Department of Biogeochemistry, Max Planck Institute for Marine Microbiology, Bremen, Germany

[b]MARUM Research Faculty and Department of Geoscience, University of Bremen, Bremen, Germany

[c]Biology Centre, Czech Academy of Sciences, Ceske Budejovice, Czechia

[d]Biological Micro- and Nanotechnology, Max Planck Institute for Biophysical Chemistry, Göttingen, Germany

Running Head: Revised Mass of Small Microorganisms

#Address correspondence to Jana Milucka, jmilucka@mpi-bremen.de

Keywords: carbon content, microorganisms, microbial biomass, subsurface, bacterioplankton

Supplementary Methods

Volumetric measurements of living cells with atomic force microscopy (AFM)

Living cells of *Formosa* sp. were imaged in an aquatic environment (i.e. growth medium HaHa100V) with AFM (NT-MDT, Eindhoven, The Netherlands) using silicon nitride probe (Scanasyst-fluid+, Bruker, Karlsruhe, Germany). The spring constant of the sharp AFM probes (2 nm curvature radius) ranged from 0.35 to 1.4 N/m. Cells were imaged at room temperature using the Hybrid method. Data was acquired and processed using the software Nova_Px 3.1.0.0 (NT-MDT, Eindhoven, Netherlands). Cell volumes were calculated by applying watershed algorithm to 3D AFM scans.

Dry mass measurements of living cells with suspended microchannel resonator (SMR)

Mass measurements of living cells of *Muricauda* sp. were conducted as follows. Living cells of *Muricauda* sp. were transferred from their incubation vial (Hungate tube) into Eppendorf tubes in which they were subsequently centrifuged (3000 g, 5 min). The pellet was resuspended in deuterium oxide-based marine broth and the cell suspension was used for SMR mass measurements. The data were collected and processed as described in main text.

Supplementary Table

Table S1. Overview of median volumes (including SE) and the variability (in %) for all measured prokaryotic species.

The variability in the cellular biovolume (in %) was defined as standard error (SE) over the median and calculated according to the formula: variability $= \frac{SE}{MEDIAN} \times 100\ \%$.

Strain name	Median V (μm^3)	Standard error V (μm^3)	Variability (%)
Nitrosopumilus sp.	0.011	0.001	11
Formosa sp.	0.023	0.002	12
Lentimonas sp.	0.025	0.005	5
Muricauda sp.	0.042	0.002	21
Maribacter sp.	0.065	0.005	13
Cellulophaga sp.	0.097	0.005	19
Lacinutrix sp.	0.106	0.006	18
Methyloceanibacter methanicus	0.119	0.005	23
Methyloceanibacter caenitepidi	0.145	0.008	18
Nitrotoga fabula	0.166	0.006	28
Kuenenia stuttgartiensis	0.238	0.008	30
Methyloceanibacter stevinii	0.705	0.035	20

Supplementary Figures

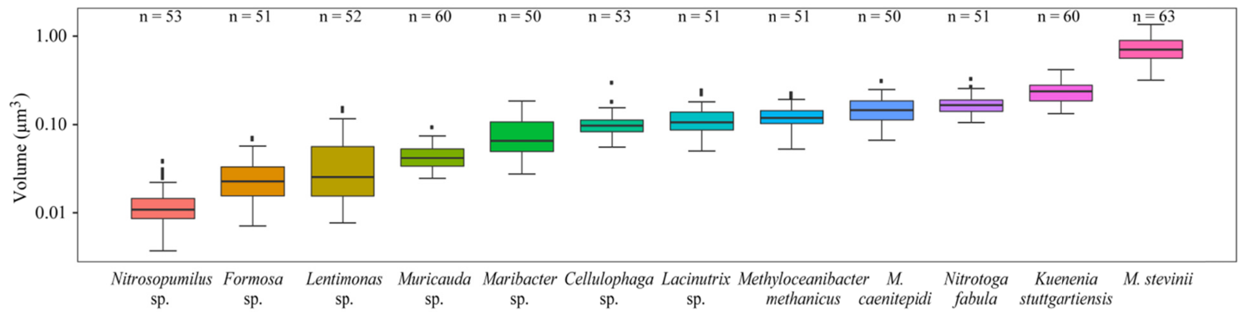

Fig. S1. Volume distributions of twelve investigated bacterial and archaeal species calculated from scanning electron micrographs (Figure 1). The volume distributions were estimated as described in the Materials and Methods and presented in forms of boxes indicating the 25th and 75th percentiles; error bars represent 10th and 90th percentiles, the lines indicate median volumes, outliers are displayed as dots. Color coding of the individual box plots corresponds to the color coding of the investigated species outlined in Figure 2. The number (n) of measured individual cells is specified above each box. The y-axis represents log-scale of volumes expressed in μm^3.

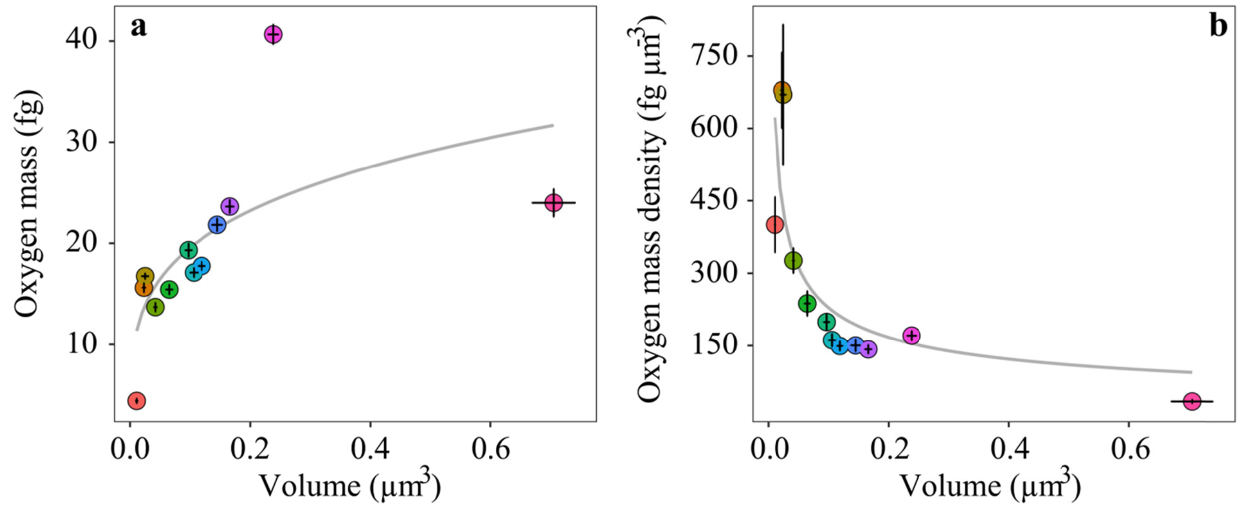

Fig. S2. Oxygen mass scaling to cellular volume for the investigated bacterial and archaeal species. Displayed is (**a**) the weak nonlinear relationship between cellular volume and oxygen mass ($R^2 = 0.48$), and (**b**) the significant (Chi-square ANOVA, P < 0.05) nonlinear relationship between cellular volume and oxygen mass density (oxygen mass per unit cell volume, $R^2 = 0.62$). The grey lines represent best fits, described by the equations: $m_{oxygen} = 35 \times V^{0.25}$ and $\rho_{m_oxygen} = 80 \times V^{-0.45}$, where m_{oxygen}, ρ_{m_oxygen}, and V are oxygen mass in fg, oxygen mass density in fg/µm^3 and volume in µm^3 respectively. Error bars indicate standard error.

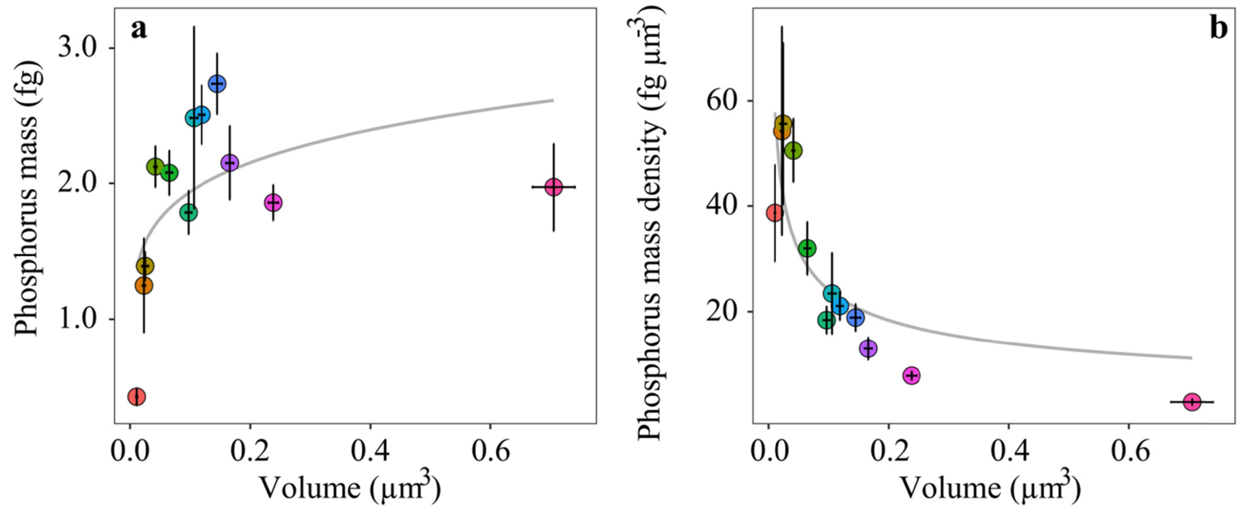

Fig. S3. Phosphorus mass scaling to cellular volume for the investigated bacterial and archaeal species. Displayed is (**a**) the weak nonlinear relationship between cellular volume and phosphorus mass ($R^2 = 0.35$), and (**b**) the significant (Chi-square ANOVA, P < 0.005) nonlinear relationship between cellular volume and phosphorus mass density (phosphorus mass per unit cell volume, $R^2 = 0.66$). The grey lines represent best fits, described by the equations: $m_{phosphorus} = 2.8 \times V^{0.15}$, $\rho_{m_phosphorus} = 10 \times V^{-0.4}$, where $m_{phosphorus}$, $\rho_{m_phosphorus}$, and V are phosphorus mass in fg, phosphorus mass density in fg/µm^3 and volume in µm^3 respectively. Error bars indicate standard error.

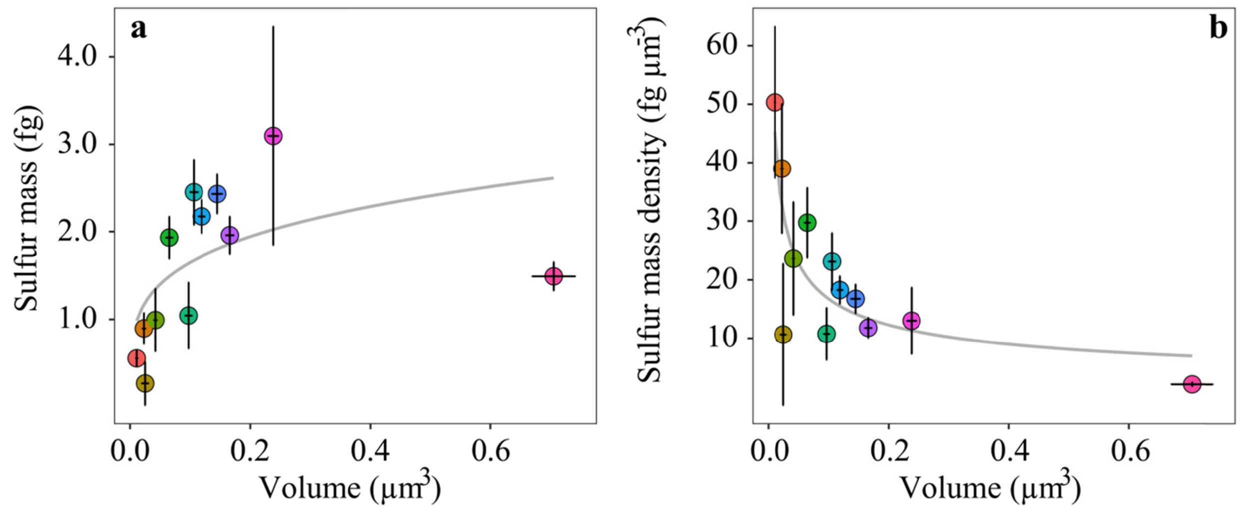

Fig. S4. Sulfur mass scaling to cellular volume for the investigated bacterial and archaeal species. Displayed is (**a**) the weak nonlinear relationships between cellular volume and sulfur mass ($R^2 = 0.35$), and (**b**) the significant (Chi-square ANOVA, P < 0.05) nonlinear relationship between cellular volume and sulfur mass density (sulfur mass per unit cell volume, $R^2 = 0.65$) for bacterial/archaeal species. The grey lines represent best fits, described by the equations: $m_{sulfur} = 2.8 \times V^{0.24}$, $\rho_{m_sulfur} = 6 \times V^{-0.45}$, where m_{sulfur}, ρ_{m_sulfur}, and V are sulfur mass in fg, sulfur mass density in fg/μm^3 and volume in μm^3 respectively. Error bars indicate standard error.

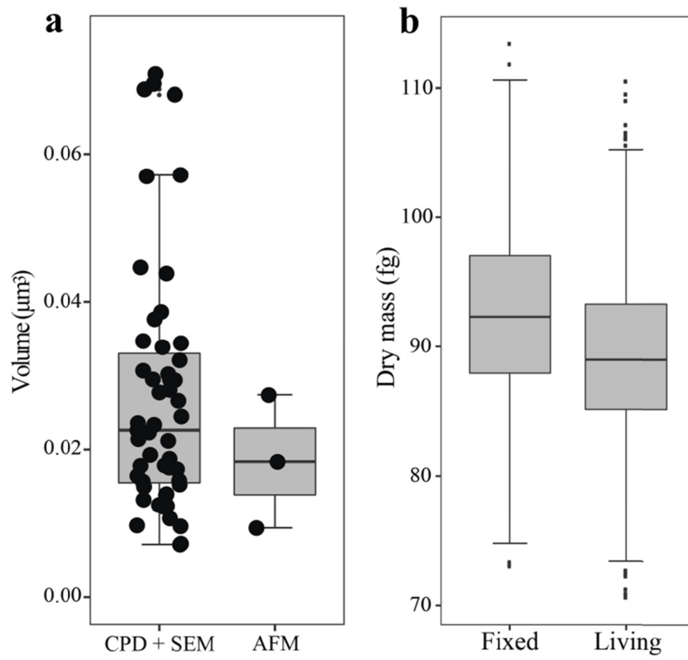

Fig. S5. Comparison of cell volume (a) and dry mass (b) between living and fixed cells. (**a**) Displayed is the range of cell volumes determined for *Formosa* sp. measured on fixed, CPD-dried and SEM-images cells (n=50) compared to live, hydrated, AFM-imaged cells (n=3). (**b**) Shown is the range of cell dry mass determined for *Muricauda* sp. when measured on fixed (n ~ 1000) and living (n ~ 1000) cells.